

DARK CURRENT STUDIES FOR SWISSFEL

F. Le Pimpec, R. Zennaro, S. Reiche, A. Adelman
 Paul Scherrer Institut, 5232 Villigen, Switzerland
 B. Grigoryan
 CANDLE Yerevan, Armenia

Abstract

Activation of the surrounding of an accelerator must be quantified and those data provided to the official agencies. This is a necessary step in obtaining the appropriate authorization to operate such accelerator. The SwissFEL, being a 4th generation light source, will produce more accelerated charges, which are dumped or lost, than any conventional 3rd generation light source, like the Swiss Light Source. We have simulated the propagation of a dark current beam produced in the photoelectron gun using tracking codes like ASTRA and Elegant for the current layout of the SwissFEL. Detailed experimental study have been carried out at the SwissFEL test facilities at PSI (C-Band RF Stand and SwissFEL Injector Test Facility), in order to provide necessary input data for detailed study of components using the simulation code OPAL. A summary of these studies are presented.

DARK CURRENT SIMULATIONS FOR SWISSFEL

The dark current is initially emitted by field emission from the photocathode, in an RF gun, and around the irises of the cavities for all accelerating RF structures. The direction of propagation of the electrons obviously depends of the RF phase and the efficiency of propagation depends of the type of cavity, traveling or standing wave (TW, SW). Impinging electrons to the surrounding walls of the cavity will produce secondaries which can also be transported along the beam line and add to the dark current.

ASTRA simulations

We have simulated the dark current of the SwissFEL [1] S-band standing wave photogun to the end of the second 4 m long S-band traveling wave structure, by using the tracking code ASTRA [2]. The initial electron bunch was produced by using the SwissFEL nominal bunch and by spreading its dimension in time and space. The emission time was limited to 120 ps which is only covering one RF bucket $\pm 60^\circ$ around the on-crest phase. We turned off the space charge option. The dark current is in reality emitted at some threshold and at every RF bucket. This simple approximation is sufficient as every other dark current bucket propagating downstream of the RF gun will be transported identically by the machine optics. From the initial 300 k particles of the bunch, $\sim 22\%$ are lost on the cathode. The losses on the walls (in percent) are quantified along the first 13 m of the machine using the remaining ~ 234 k particles,

Fig.1. Only 9.7% of those remaining particles reach the beginning of the third S-band accelerating structures. As shown in Fig.1, more than 90% of the bunch is lost before even reaching the first S-band structure with a ~ 7 MeV kinetic energy. The 9.7% remaining particles are concentrated in the core of the initial bunch. The output distribution was reused as an input for the elegant tracker [3] from the beginning of the third S-band structure.

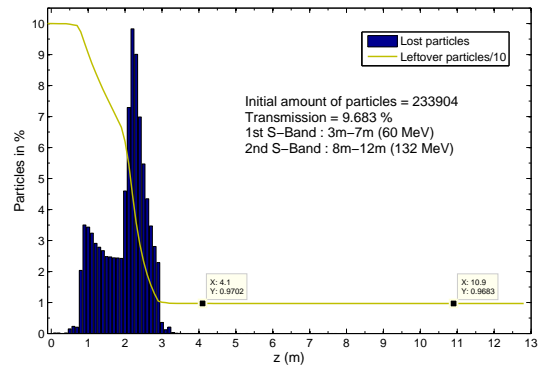


Figure 1: Histogram of the particle losses at the walls of the accelerator up to the end of the second S-band cavity (132 MeV). The continuous line represents the surviving particles in percent ($/10$) of the initial remaining particles.

Elegant simulations

The left over particles from the ASTRA simulation were not numerous enough to do a proper elegant simulation. We have multiplied the input distribution by cloning every particle with a small change in their positions and momenta. We hence produced 2.2 million particles. The tracking was done using the SwissFEL Elegant model which includes the physical apertures of the machine and by adding three particle collimators toward the end of the Aramis beam line [1]. The space charge and wake field options were turned off. Fig.2 shows at which location some particles are lost and with which energy and energy spread. The energy spread for the lost particles is small, less than 1%, as can be seen by the small error bars displayed in the bottom plot of Fig.2. Losses are concentrated before the first bunch compressor ($s \sim 50$ m) and at the second bunch compressor ($s \sim 200$ m), as shown by Fig.3. No other losses are recorded after the second bunch compressor. The transverse collimators placed at the end of the machine

($s > 400$ m) induce dark current losses only for apertures smaller than 2 mm in radius.

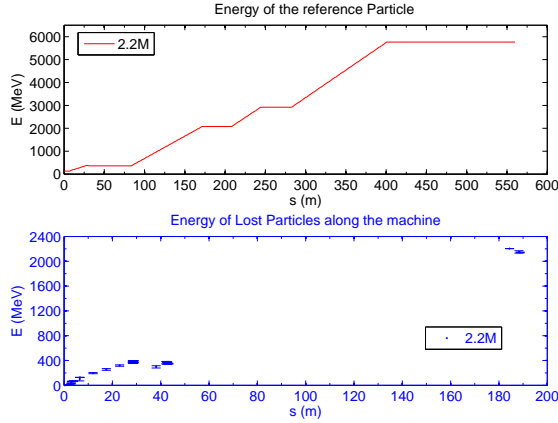


Figure 2: Top: Energy gained by the reference particle up to the end of the Aramis beam line. Bottom: Average energy and the standard deviation of the lost particles along the machine.

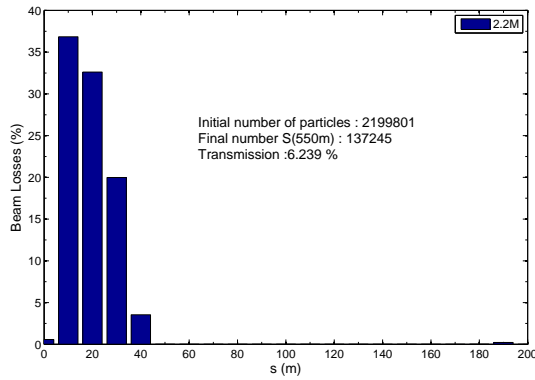


Figure 3: Histogram of the particle losses at the walls of the accelerator up to the end of the Aramis beam line (6 GeV)

Further simulations were carried out to find out the effects of different acceleration schemes, due to potential SwissFEL operation conditions. The case presented uses the full acceleration in LINAC 3 up to ~ 6 GeV. Other cases using a deceleration to 2.1 GeV at the entrance of LINAC 3, a deceleration to 2.1 GeV at the end of LINAC 3 shows no differences in losses for the same aperture of the collimators. Small Difference arise for collimator sizes below the 2 mm radius. LINAC 3 is the last stage of acceleration for the hard X-ray beamline. It raises the beam energy from ~ 3 GeV to 6 GeV. This linac starts downstream of the beamline switchyard at $s \approx 280$ m). More details about the layout of the machine can be found in reference [1]

Finally, we used elegant to track back some potential dark current produced by the TW C-band RF structures [4]. In a TW structure the RF capture phase exists only in the direction of propagation of the RF wave. Due to the design

of our C-band structure, we do not expect any dark current above a few MeV traveling upstream of the LINAC. In elegant reversing the linac model will also reverse the direction of propagation of the RF hence allowing captures of an upstream propagating electron beam. Despite this limitation, we find that no dark current produced by the last C-band structure of LINAC 3 makes it back to the beginning of the machine for an initial electron energy below 25 MeV. This energy exceed by far the energy gained by electrons accelerated through 2 or 3 cells in a structure.

OPAL simulations

The preceding simulations have been carried out by using a blown up bunch based on the initial SwissFEL bunch. In order to use a more adequate bunch distribution, we have used the dark current module from OPAL [5], turning off the secondary electron emission switch. We have tested the emission and propagation of a dark current beam using a Fowler-Nordheim (FN) threshold for emission of 40 MV/m and a FN enhancement factor β of 80. For the component simulation, we have used the actual layout of the SwissFEL injector gun, labeled CTF3 in Fig.4 [6]. The CTF3 gun is a two and a half cell SW RF structure. The RF field at $t=0$ ps is 100 MV/m on axis. For every picosecond the RF phase changes by 1° . The electrons are created at first on the cathode side and on the downstream side of the irises and electrons start propagating downstream of the beam line. 180° later the electrons are created in the upstream side of the irises and start propagating upstream (toward the cathode). Fig.4 shows a snapshot at $t=545$ ps of the propagation of the electrons. The 6D phase space output of the simulation can be used as an input for the OPAL or elegant trackers. The modified module also handle TW structures. We are planning to simulate the dark current production from an actual C-band test structure [4].

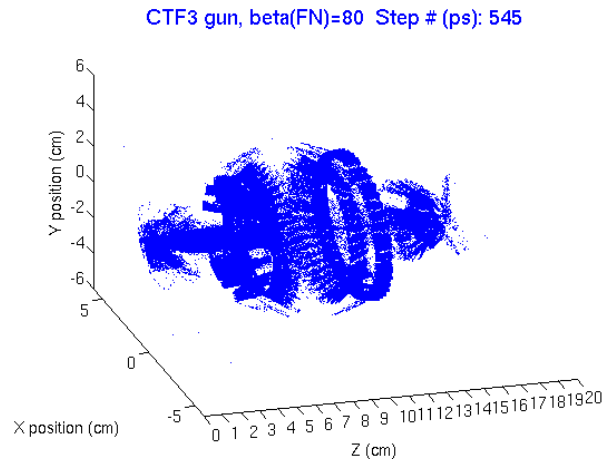


Figure 4: Propagation of the dark current in a SW photo-gun. The electron propagates upstream toward the cathode and downstream toward the exit of the gun

EXPERIMENTAL RESULTS AT VARIOUS SWISSFEL FACILITIES

Dark current at the SwissFEL injector

In order to provide proper inputs for the simulation we measured the dark current produced by the injector RF photogun (CTF3), and by the 4 m long S-band TW structure. Its propagation along the beamline was also studied [6]. The CTF3 gun produces around 6 nC of dark current at nominal power (100 MV/m accelerating gradient). The charge is measured using the wall current monitor (WCM) located downstream of the gun. The emission of dark current in the gun is FN driven, as shown by the left plot in Fig.5. Using equation.1 [7], we have extracted the FN enhancement factor $\beta = 78$ for such structure, Fig.5 (right plot).

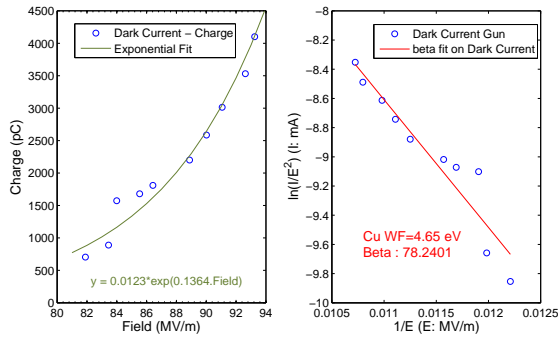


Figure 5: Left: CTF3 gun charge emission vs accelerating field. Right: Enhancement factor β determination.

$$\beta = \frac{6.83 \cdot 10^3 \times \Phi^{\frac{3}{2}}}{k_2} \quad (1)$$

Where $\Phi = 4.65 \text{ eV}$ is the work function, and k_2 is the slope of the fit. Warm RF cavities with β of ~ 50 are usually consider good structures.

In order to determine the energy spread of the dark current we have used two techniques. In one case, we have varied the input power at the gun and looked at the beam at the screen located at the dump of the energy spectrometer. In the other case, we swept the beam on the screen using the spectrometer dipole at nominal power. We measured a threshold for dark current at 4.3 MeV and a maximum energy of 7.2 MeV. The dark current energy on the lowest end could be lower than the measured 4.3 MeV, but we could not detect any electrons neither on the WCM nor on any scintillating screens of the beamline.

We have measured the dark current coming from the third TW S-band structure with 28 MW input power (17 MV/m). We did not observed any dark current on either upstream or downstream screens. We estimated the dark current charge transmitted through the machine to be $\sim 18 \text{ pC}$. Radiation measurement performed at the injector were in qualitative agreement with the ASTRA results, a

peak of radiation is measured at the entrance of the first TW S-band structure.

Dark current of a C-band test structure

The main acceleration of the SwissFEL will be provided by C-band structures with an RF pulse of 350 ns flat top at 28 MV/m [1]. It is of importance to test not only the quality of the mechanical production of such structures, but also their RF properties [4]. A small prototype has been RF tested and its dark current measured using the 2 Faraday cups (FCs) installed at each end of the beamline Fig.6. For the coming structures an Integrated Current Transformer (ICT) [8] will be installed in the beamline.

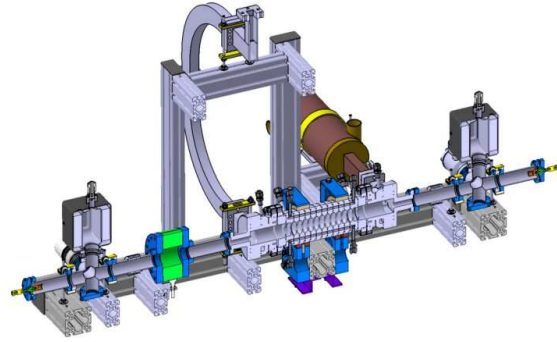


Figure 6: C-Band TW structure test stand, showing a faraday cup at each end of the beam line and an ICT.

We did not record any dark current on either the upstream or downstream FCs by running the C-band cavity for hours at an accelerating gradient of 38 MV/m, hence 10 MV/m above the design value, and with a 350 ns RF flat top pulse. This amounts for $\sim 51 \text{ MW}$ of input power. Dark current were solely detected during breakdowns. Breakdowns were produced by increasing the input power by a few MW above 51 MW. The use of an X-ray scintillator [9], placed 1 m away from the structure, proves that the dark current exists inside the structure. Using the NIST [10] database, we determined that photons $> 300 \text{ keV}$ can make it through 20 mm of Cu. At 38 MV/m on axis field, an electron in 1 cell (2 cm) can acquire up to 750 keV. The X-ray signals is well fitted by the use of an exponential function, as expected for dark current coming from field emission, Fig.7.

Using equation.1 and assuming that the integrated x-ray signal is proportional to the dark current, we estimated that the FN β is 68.

CONCLUSIONS

In order to obtain the necessary official authorization to operate SwissFEL, the production of radiation along the machine must be quantified. We have produced a first set of simulations results using ASTRA, elegant and OPAL as

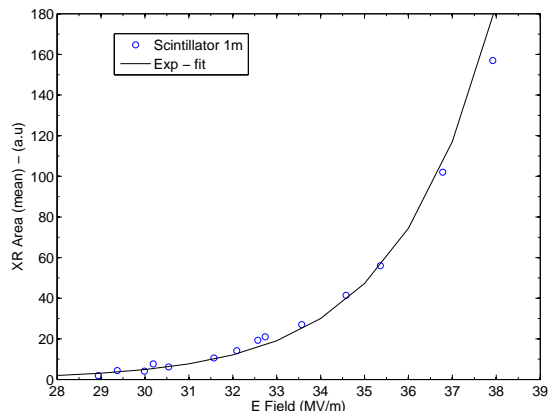


Figure 7: X-ray signal in function of the Electric Field inside the C-Band TW structure. The curve shows a FN type electron emission.

well as carrying out real measurements at two SwissFEL facilities. The outcomes are :

- * Like in many other facilities around the world, the dark current is essentially produced by the SW photogun.
- * Most of the dark current is lost at the first S-band structure.
- * The remaining of it is mostly lost before the first bunch compressor.
- * Only a small fraction of the dark current, mainly its core produced at the photocathode, goes to the end of SwissFEL.
- * At nominal power, neither the S-band nor the C-band test structures produce any measurable dark current, although electrons are present in the structures.

Finally, we are continuing the dark current investigation on subsequent C-band structures, by installing closer from the exit/entrance of the structure an ICT for a more sensitive detection of electrons. We are also planning to measure the spectrum of the X-rays emitted during the RF pulse to obtain the maximum energy that electrons in the structure have achieved. We will run OPAL using the C-band test structure geometry and use the X-ray data to cross check the validity of the simulations.

ACKNOWLEDGMENTS

We would like to thank A. Citterio and A. Jurgens for their help at the C-band test facility. The lead author is indebted to his beam dynamic colleagues for their various help. We also acknowledge the help of C. Wang (CIAE, China) for modifying OPAL according to our needs. We also thank the radiation protection group for their support of this work.

REFERENCES

- [1] R. Ganter, editor. *SwissFEL Conceptual Design Report*. PSI-10-04. 2012.
- [2] K. Flöttmann. A Space Charge Tracking Algorithm. <http://www.desy.de/~mpyflo/>.
- [3] M. Borland. elegant: A Flexible SDDS-Compliant Code for Accelerator Simulation. Advanced Photon Source LS-287, September 2000.
- [4] R. Zennaro, J. Alex, H. Blumer, M. Bopp, A. Citterio, T. Kleeb, L. Paly, J.-Y. Raguin. Design Construction and power conditioning of the first C-band accelerating structure for SwissFEL. In *IPAC12, New Orleans, USA, 2012*.
- [5] A. Adelman. OPAL : Object Oriented Parallel Accelerator Library. <http://amas.web.psi.ch/docs/opal/html/index.html>.
- [6] M. Pedrozzi, editor. *SwissFEL Injector Conceptual Design Report*. PSI-10-05. 2010.
- [7] F. Le Pimpec, C. Gough, V. Chouhan, S. Kato. Field emission from carbon nanotubes in DC and pulsed mode. *Nuclear Instruments and Methods in Physics Research A*, 660:7–14, 2011.
- [8] Bergoz Instrumentation. <http://www.bergoz.com/>.
- [9] F. Le Pimpec et al. Results of the PSI Diode-RF Gun Test Stand Operation. In *IPAC2010, Kyoto, Japan, 2010*.
- [10] http://www.nist.gov/pml/data/xray_gamma.cfm.